Pergamon

Electrochimica Acta, Vol. 43, Nos 3–4, pp. 315–324, 1998

Printed in Great Britain
PII: S0013-4686(97)00072-8
0013-4686/98 $19.00 + 0.00

Process aspects of the electrolytic codeposition of molybdenum disulfide with nickel

Yu-Chi Chang,[a]* Ying-Yin Chang[b] and Chun-I Lin[b]

[a]Department of Chemical Engineering, Tamkang University, Tamsui, Taipei Hsien, Taiwan 25137, R.O.C.
[b]Department of Chemical Engineering, National Taiwan Institute of Technology, Taipei, Taiwan 106, R.O.C.

(Received 7 October 1996; in revised form 2 January 1997)

Abstract—Process characteristics of the electrolytic codeposition of molybdenum disulfide particles with nickel from a Watts bath have been analysed in this study using statistical experimental design. The results show that temperature and concentration of suspended particles significantly affect the weight percentage of molybdenum disulfide in the deposit. Particle concentration has a positive effect, while temperature exerts an adverse effect. Moreover, pH and temperature have been observed to be significant factors affecting the nickel deposition efficiency. Both factors exert positive effects. A second order model, relating the current efficiency to pH and temperature, has been developed. This model adequately approximates the performance measures. The physical model proposed by Guglielmi has been shown to be valid from the present system at low current densities. The results at high current densities, however, show different features. It has also been observed that the presence of particles affects the nickel reduction reaction in an unknown way. © 1997 Elsevier Science Ltd

Key words: composite electrodeposition, Ni—MoS_2, Guglielmi's model, response contours.

INTRODUCTION

Composite electrodeposition, consisting of inert solid particles embedded in metallic matrix, has been developed in recent years for various applications. However, the insights into the mechanisms behind the codeposition process have grown at a much slower pace than the applications of the composite coatings. Theories pertaining to the mechanisms of capture and encapsulation of particles during metal deposition have only begun to be developed in the last few years [1]. The models developed by Guglielmi [2], Celis *et al.* [3], and Fransaer *et al.* [4] provide a better theoretical insight into the codeposition process. Several excellent review papers concerning electrolytic codeposition have been published in recent years [5, 6]. In-depth understanding of the codeposition mechanism is very important, since it can help to control the plating structure, and consequently the plating properties. Unfortunately, the present understanding of the mechanism of electrolytic codeposition is not sufficient to predict the effects of variations in electrolysis conditions on the resulting codeposition. Further studies are necessary to determine the influence of plating variables on the resulting codepositions, so that the mechanisms behind codeposition may be understood more completely.

Molybdenum disulfide is often dispersed in metal matrices like copper and nickel to achieve enhanced strength of the final composite material for good wear resistance [7]. Recently, it has been pointed out that molybdenum disulfide-coatings can be used as appropriate hydrogen evolution catalysts, provided there exists an easy way to prepare and apply them [8]. Towards this end, Chang has recently prepared the nickel–molybdenum disulfide composite by composite electrodeposition and has examined its electrocatalytic properties in alkaline electrolytes [9].

The plating variables which are likely to be important towards controlling the degree of particle incorporation in the deposit include the metal to be plated, composition of the plating bath, pH of the

*Author to whom correspondence should be addressed.

bath, composition of the non-metallic phase, size and shape of the non-metallic particles, current density, current form and stirring efficiency [10]. Ghouse *et al.* [11] have studied the effects of pH (1.5 and 5.5), current density (25–100 mA/cm^2) and particle concentration (1–50 g/dm^3) on the extent of incorporation of MoS_2 in the Ni—MoS_2 composites, prepared by the conventional electrodeposition and sediment codeposition techniques using the Watts type bath as electrolyte. The influence of current density (25–100 mA/cm^2) and particle concentration (1–50 g/dm^3) on the percentage of the MoS_2 particles incorporated in the Cu—MoS_2 system using copper sulfate bath as electrolyte have also been studied [7]. The effects of pH, current density, particle concentration and temperature on the effectiveness of molybdenum disulfide incorporation in the nickel–molybdenum disulfide composite prepared by sediment codeposition technique by using the fluoborate bath as the electrolyte have also been reported [12]. The extent to which the inert solid particles can be incorporated, however, depends on the nature of the system. For instance, increasing the current density has an adverse effect on the percentage of the molybdenum disulfide particles incorporated in the Ni—MoS_2 system [11], whereas incorporation of the same particles increases up to a critical current density in the Cu—MoS_2 system [7]. Sautter [13] has reported that there is no effect of temperature on the codeposition of Al_2O_3 with nickel from a Watts type bath, whereas Bapu [12] has reported that temperature severely affects the incorporation of MoS_2 in the Ni—MoS_2 system. Therefore, it is important properly to characterize the basic plating parameters that affect the incorporation of solid particles into the deposit, for specific systems.

The process characteristics of electrocodeposition of molybdenum disulfide particles and nickel metal are far from being well understood. The present investigation therefore aims systematically to study the effects of various plating bath variables on the amount of molybdenum disulfide codeposited with nickel from the Watts bath and the current efficiency of the electrolytic process. Further, the relative importance of these variables has been judged from the present experimental findings by carrying out the statistical analysis. The applicability of Guglielmi's model to the nickel–molybdenum disulfide composite electrodeposition system has also been studied.

EXPERIMENTAL

The nickel–molybdenum disulfide composite coatings were prepared on copper substrate by the rotating disc electrode technique with external auxiliary stirring, using a Watts type bath as the electrolyte. The basic bath composition was: $NiSO_4 \cdot 7H_2O$, 310 kg/m^3; $NiCl_2 \cdot 6H_2O$, 50 kg/m^3; and H_3BO_3, 40 kg/m^3. Concentrations of MoS_2 particles ranging from 10–50 kg/m^3 were added to the bath. It deserves mention that in all cases, bath pH decreased (values ranged from 0.1 to 0.3) with the introduction of MoS_2 particles. Solution pH was adjusted with H_2SO_4 prior to each deposition. The size of MoS_2 particles was less than 2 microns. The electrolyte was prepared from reagent grade chemicals and deionized water. 50 cm^3 solution was used for each experiment. A copper disc of 0.9 cm in diameter formed the working electrode, whereas platinum gauze formed the anode. The disc electrode was embedded into a cylindrical Teflon base of 1.5 cm diameter. A hot plate with magnetic stirring facility was used for heating and stirring the bath.

In order to prevent agglomeration of particles and to obtain uniform dispersion of molybdenum disulfide in the bath, the required amount of MoS_2 powder was first thoroughly blended with a small quantity of wetting agent sodium lauryl sulfate (in 1 M concentration, 0.4 cm^3 SLS/g MoS_2) in the reactor, a small amount of electrolyte (8 cm^3) was then added to make a slurry, and the remaining electrolyte was finally added to the resulting slurry. The particles were kept suspended in the solution by a magnetic stirrer and electrocodeposition was performed galvanostatically for the required period of time. The product of the current times the electrolysis time gives the number of coulombs, which was 56.55 C for each experiment. The theoretical thickness of the coating was 31 microns for the corresponding reaction of nickel deposition with 100% current efficiency. The actual thickness of the electrodeposited composites varied with electrolytic conditions.

A survey of relevant literature reveals that process variables (factors) that are likely to be important in affecting the composition of the deposit and current efficiency are: particle concentration, current density, pH, temperature and hydrodynamic conditions. An approach for studying the effects of these parameters by one-factor-at-a-time experimentation is certainly ineffective. Since the number of parameters involved is large, a fractional factorial design is an effective way to identify the influential factors in a systematic fashion [14]. Moreover, in some chemically reacting systems the difference in response (the performance measure) between particular levels of one factor is not the same at all levels of the other factors, indicating a significant interaction between various factors. Such significant interaction might even sometimes mask the significance of main effects. A factorial design, in this regard, is necessary when such interactions are present, in order to avoid misleading conclusions.

Table 1 shows the 27-run 3^{13} design used in the present investigation, the columns indicating the actual effects that they estimate. The last two columns show the experimentally determined percentage of MoS_2 incorporated in the deposit and the current efficiency of the electrolytic codeposition, respectively. Randomization was employed in conducting

Table 1.
Design of the nickel–molybdenum disulfide electrocodeposition experiment

Run	Test sequence	*A*	*B*	*AB*	*AB*	*C*	*AC*	*AC*	*AD*	*D*	*AD*	*AF*	*F*	*AF*	MoS_2% (deposit)	Current efficiency (%)
1	21	1	1	1	1	1	1	1	1	1	1	1	1	1	40.2	27.81
2	5	1	1	1	1	2	2	2	2	2	2	2	2	2	13.6	58.27
3	16	1	1	1	1	3	3	3	3	3	3	3	3	3	12.1	85.25
4	11	1	2	2	2	1	1	1	2	2	2	3	3	3	29.4	62.80
5	22	1	2	2	2	2	2	2	3	3	3	1	1	1	29.8	68.16
6	9	1	2	2	2	3	3	3	1	1	1	2	2	2	38.8	23.13
7	1	1	3	3	3	1	1	1	3	3	3	2	2	2	13.0	61.71
8	15	1	3	3	3	2	2	2	1	1	1	3	3	3	17.1	53.98
9	26	1	3	3	3	3	3	3	2	2	2	1	1	1	54.8	15.77
10	2	2	1	2	3	1	2	3	1	2	3	1	2	3	12.9	44.56
11	13	2	1	2	3	2	3	1	2	3	1	2	3	1	19.7	91.97
12	27	2	1	2	3	3	1	2	3	1	2	3	1	2	52.9	25.47
13	19	2	2	3	1	1	2	3	2	3	1	3	1	2	32.0	83.81
14	6	2	2	3	1	2	3	1	3	1	2	1	2	3	30.7	15.31
15	17	2	2	3	1	3	1	2	1	2	3	2	3	1	17.3	68.76
16	12	2	3	1	2	1	2	3	3	1	2	2	3	1	14.7	69.43
17	23	2	3	1	2	2	3	1	1	2	3	3	1	2	34.1	56.70
18	7	2	3	1	2	3	1	2	2	3	1	1	2	3	24.4	94.94
19	10	3	1	3	2	1	3	2	1	3	2	1	3	2	22.0	49.88
20	24	3	1	3	2	2	1	3	2	1	3	2	1	3	20.5	37.90
21	8	3	1	3	2	3	2	1	3	2	1	3	2	1	19.7	56.02
22	3	3	2	1	3	1	3	2	2	1	3	3	2	1	21.4	55.29
23	14	3	2	1	3	2	1	3	3	2	1	1	3	2	16.7	94.44
24	25	3	2	1	3	3	2	1	1	3	2	2	1	3	42.2	62.17
25	20	3	3	2	1	1	3	2	3	2	1	2	1	3	30.9	10.45
26	4	3	3	2	1	2	1	3	1	3	2	3	2	1	27.3	66.78
27	18	3	3	2	1	3	2	1	2	1	3	1	3	2	51.6	14.91

the experiments, in order to spread the effect of unknown nuisance variables across the entire experimental region. The factors and their respective magnitudes used in the experiments are presented in Table 2. The quantitative determination of molybdenum disulfide embedded in the nickel matrix was carried out by XRD analysis [9]. The disc samples were rinsed thoroughly by deionized water and were dried at 323 K before being analysed. The reported composition is the weight percent of MoS_2 particles incorporated into the film, whereas the current efficiency is defined as percentage of the total applied charge that results in the deposition of nickel metal.

Table 2.
Experimental conditions employed in this study

Factor	Level 1	Level 2	Level 3	Unit
A: current density	100	200	400	A/m^2
B: rotation rate	500	1000	1500	r.p.m.
C: particle concentration	10	25	50	kg/m^3
D: pH	0.5	2.0	4.0	
F: temperature	298	313	328	K

RESULTS AND DISCUSSION

Process characteristics

A major application of fractional factorials is in the screening experiments. Since a large number of factors usually includes parameters that do not significantly affect the response measure, the screening process provides an efficient way to remove such

Table 3.
Analysis of variance for the MoS_2 wt.% experiment

Source of variation	Degrees of freedom	Mean square (*10^4) (MSB)	F_0 (=MSB/MSE)
A	2	5.57	—
B	2	92.94	—
C	2	378.43	5.38*
D	2	141.20	2.01
F	2	686.58	9.77*
AB	4	99.20	—
AC	4	62.44	—
AD	4	111.40	1.58
AF	4	114.04	1.62

Mean Square Error (MSE) = (*A*,*B*,*AB*,*AC*) = 70.30.

unimportant factors from consideration. The factors that are identified as important are then investigated more thoroughly in the subsequent experiments. Table 3 summarizes the analysis of variance for the percentage of MoS_2 incorporated in the deposit. For a fixed effects model, the test statistics for each main effect and interaction can be constructed by dividing the corresponding mean square of the effect or interaction (MSB) by the mean square error (MSE). Since a single replicate of a factorial design enables no estimate of error, one approach to the analysis of an unreplicated fractional factorial is to pool certain main effects and interactions with smaller mean square to obtain an error mean square [15]. In the present study, main effects A and B and interactions AB and AC are combined to estimate the error. Since $F_{0.05}(2,12) = 3.89$ and $F_{0.05}(4,12) = 3.26$, we conclude that temperature (F) and particle concentration (C) significantly affect the weight percentage of MoS_2 in the deposit (significant at 5%). The factor D (pH) and interactions AD (current density–pH) and AF (current density–temperature) are, however, of no major concern.

The analysis of variance for the current efficiency data is presented in Table 4. The mean square error has been computed by the same method described previously. Here B, C, AC and AF are pooled to obtain the error mean square. The conclusion that one can draw from this analysis is that pH(D) and temperature (F) are significant at the 5 percent level since $F_{0.05}(2,12) = 3.89$ and $F_{0.05}(4,12) = 3.26$, while the current density–rotation rate interaction (AB) is significant at the 10 percent level ($F_{0.10}(4,12) = 2.48$), indicating a mild interaction between these factors.

To assist in practical interpretation of the above results, Fig. 1 presents plots of the five main effects for the MoS_2 wt.% data, wherein the magnitude of main effect refers to the change in response produced by a change in the level (magnitude) of the factor. These main effect plots are just graphs of the marginal response average at the given levels of the five factors. The steepness of the slope reflects the importance of the respective effect. It should be noted that a factorial design allows the effects of a factor to be estimated at several levels of the other factors, yielding conclusions that are valid over a large range of experimental conditions.

Table 4.
Analysis of variance for the current efficiency experiment

Source of variation	Degrees of freedom	Mean square ($\times 10^4$) (MSB)	F_0 (=MSB/MSE)
A	2	362.21	1.47
B	2	226.58	—
C	2	293.61	—
D	2	3264.15	13.28*
F	2	1153.58	4.69*
AB	4	731.58	2.98*
AC	4	359.87	1.46
AD	4	226.04	—
AF	4	251.51	—

Mean square error (MSE) = (B,C,AD,AF) = 245.88.

The marginal means plot of the effects of current density is presented in Fig. 1(a), which indicates that there is essentially no difference in the weight percent of the deposit at different current densities, within the experimental range studied. This behaviour is in agreement with the results obtained by other investigators on other plating systems [7, 16], but contradicts the results of Ghouse *et al.* [11], who observed the current density to exert a slight adverse effect on the percentage of incorporation. Notably, the data reported by Ghouse *et al.* are based on the one-factor-at-a-time experimentation. It deserves mention that current density has been observed to be an unimportant factor in the present statistical analysis (Table 3).

Figure 1(b) shows the marginal means plot of the effect of rotation rate, which shows that the percentage of incorporated molybdenum disulfide particles increases slightly with increasing rotation rate of the disc electrode. Buelens *et al.* [17] have studied the codeposition of fine Al_2O_3 particles with copper by the rotating disc electrode technique and have observed a marked decrease in embedded alumina at the beginning of the transition zone and a significant increase in the quantity of embedded alumina with increasing rotation speed, until the turbulent zone is reached. Spiral contours were observed on the rotating disc cathode in the present investigation after the process of electrolytic codeposition was terminated. Appearance of spirals is sometimes related to the transition from laminar to turbulent flow [18]. The present results are therefore in agreement with those of Buelens *et al.* [17].

The marginal means plot of the effect of molybdenum disulfide particles concentration in the bath is presented in Fig. 1(c). It can be seen from this figure that weight percent of molybdenum disulfide in the deposit increases as the concentration of molybdenum disulfide increases. This suggests that the codeposition of MoS_2 depends on the number of collisions between particles and cathode. This figure also indicates that MoS_2 concentration in the bath has a significant impact on the mean response (weight percent of MoS_2 in deposit).

The marginal means plot of the effect of pH is presented in Fig. 1(d), which shows that the weight percentage of molybdenum disulfide in the deposit decrease as the pH of the bath increases. A similar observation has also been reported by Ghouse *et al.* [11]. It is possible that at lower pH, hydrogen ions preferentially adsorb on the MoS_2 particles, permitting these particles to attach themselves to the cathode, thus favoring incorporation of MoS_2 in the deposit.

Fig. 1(e) is the marginal means plot of the effect of

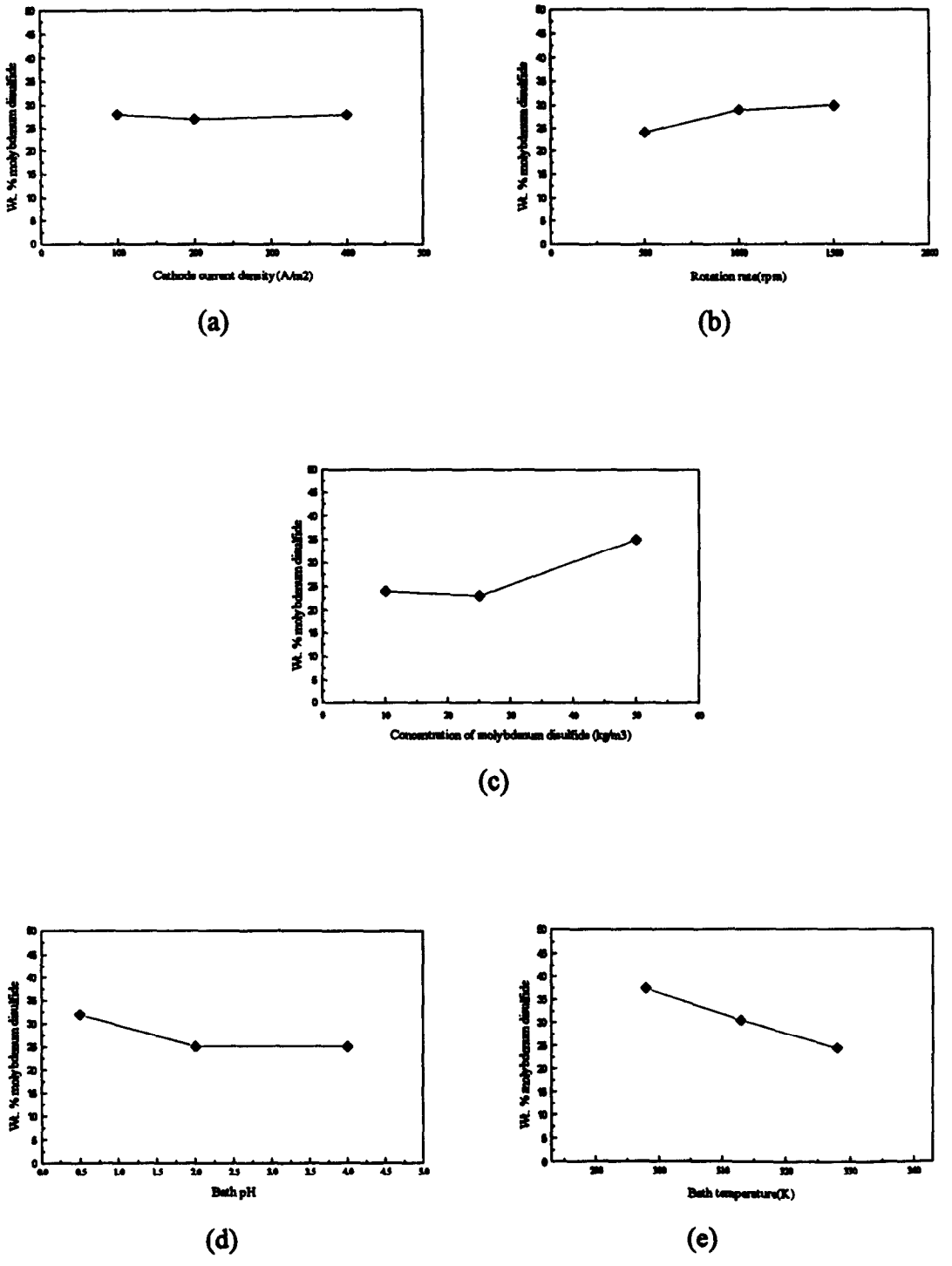

Fig. 1. Plots of the main effects for MoS_2 wt.% in deposit. (a) Current density (A). (b) Rotation rate (B). (c) MoS_2 concentration in the bath (C). (d) pH (D). (e) Temperature (F).

temperature. Variations in the temperature of the bath can be seen to exert a pronounced influence on the weight percent of MoS_2 powder in the deposit. It appears that as the temperature of the bath is increased, less powder is included in the deposit. A similar adverse effect of higher temperatures on codeposition of MoS_2 in a fluoborate bath has also been reported [12]. The effectiveness of the incorporation of particles in the deposition on cathode is dependent on the preceding process of adsorption of

ionic species onto these particles. Temperature obviously has an adverse effect on adsorption of ions onto the particles [19], thus resulting in the decrease of MoS_2 incorporation.

Current efficiency is one of the important figures of merit for the electrolysis process [20]. However, very few studies have investigated the effects of the plating variables on the efficiency of metal deposition in electrolytic codeposition. Figure 2 presents plots of the five main effects in this process. Analysis of Fig. 2 indicates that pH and temperature significantly affect the mean response (current efficiency).

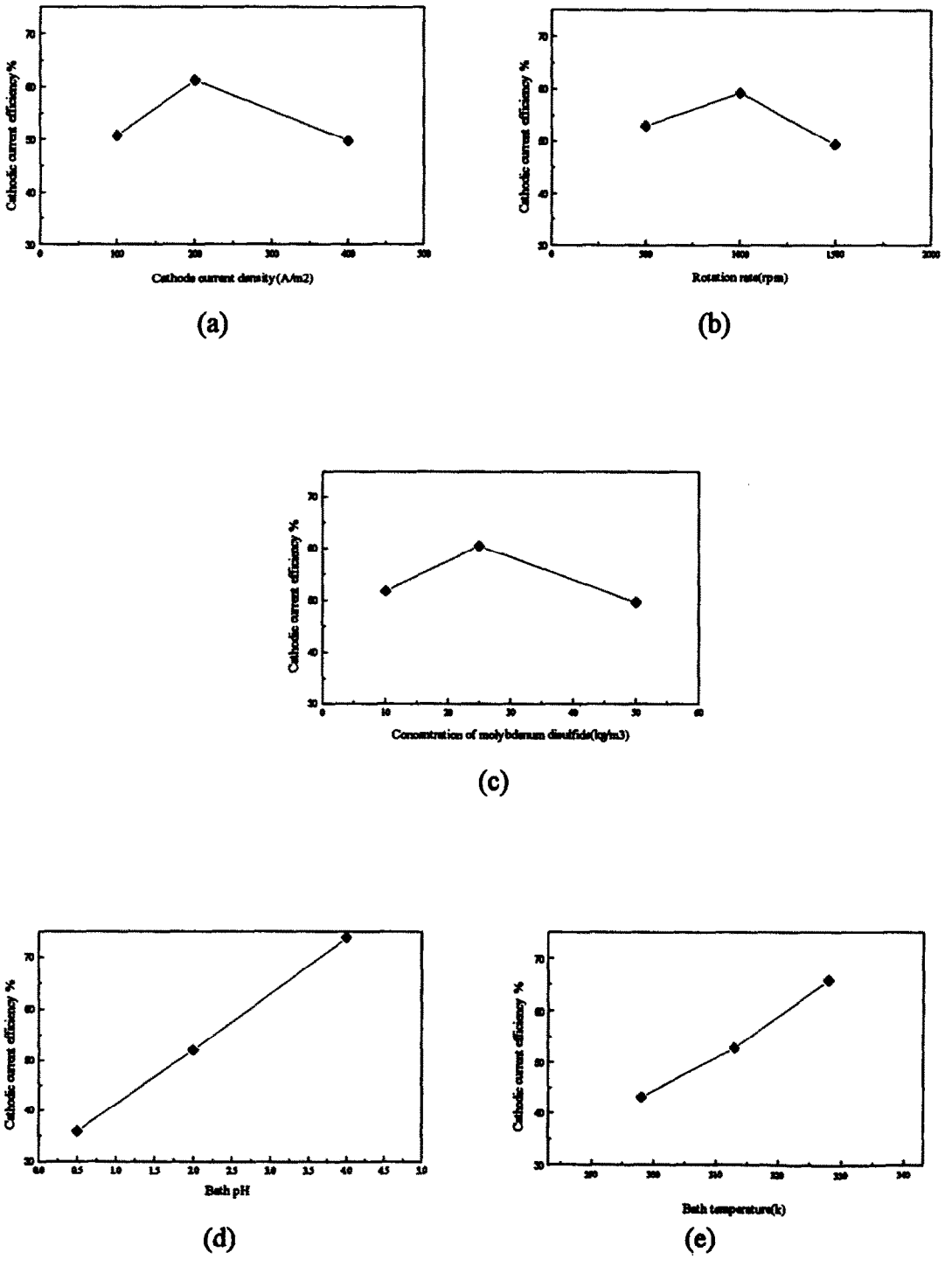

Fig. 2. Plots of the main effects for current efficiency. (a) Current density (*A*). (b) Rotation rate (*B*). (c) MoS_2 concentration in the bath (*C*). (d) pH (*D*). (e) Temperature (*F*).

Figure 2(a) shows the marginal means plot of the effect of current density. The result indicates that current efficiency increases up to a current density of 200 A/m^2 and then reduces abruptly. Such reduction in current efficiency beyond 200 A/m^2 can be explained on the basis of the polarization effect at higher current densities, leading to reduced metal deposition efficiency. However, somewhat different results have been reported for the electrodeposition of nickel from a particle-free Watts bath [21], wherein the current efficiency was observed to increase with the increase in the current density, but only at lower current densities, while an almost constant current efficiency was observed at higher current densities.

The marginal means plot of the effect of rotation rate is presented in Fig. 2(b). An increase in current efficiency is observed with increasing rotation rate until a critical rotation rate is reached, whereupon the current efficiency decreases. A comparison of this result with that in Fig. 1(b) reveals that the metal deposition efficiency decreases dramatically in the regime in which particles incorporation is greatest. Recently, Webb *et al.* [22] have investigated the electrolytic codeposition of Ni–γ-Al_2O_3 thin film and showed that the current efficiency decreases with increasing rotation rate at lower current densities (<100 A/m^2), while at higher current densities (>400 A/m^2) the current efficiency increases up to a critical rotation rate and then decreases. The present observation is thus consistent with the results obtained by Webb *et al.* It should be pointed out that such rotation rate dependence of the shifting behaviour indicates the existence of interaction between current density and rotation rate. This observation is consistent with the conclusion reached based on the statistical analysis in the present study. Notably, such current density–rotation rate interaction has not been previously documented.

The marginal means plot of the effect of MoS_2 concentration in the bath is presented in Fig. 2(c). It appears from this figure that the current efficiency initially increases and then decreases. To gain further insight on the influence of the presence of particles on metal current efficiency, nickel deposition experiments were performed on particle-free and particle-containing systems. Results of these experiments are given in Table 5. It is clear that presence of MoS_2 particles affects the nickel deposition efficiency in some way, since the nickel deposition efficiency has been observed to be reduced by the presence of molybdenum disulfide particles in the bath.

Figure 2(d) shows the marginal means plot of the effect of pH. The current efficiency appears to increase as the pH of the bath increases. This increase in nickel deposition efficiency with increasing pH can be attributed to the suppression of the competing hydrogen evolution reaction. Examination of the surface morphology of the disc surface with a scanning electron microscope revealed that a more porous surface is produced from electrolytes with higher acid contents. This observation thus explains the observed changes in current efficiency as a function of pH.

Table 5.
Effect of MoS_2 particles on nickel depostion efficiency

Run	Test sequence	Currency efficiency (%) With MoS_2	Currency efficiency (%) MoS_2 free
14	1	15.31	15.69
4	2	62.80	70.35
11	3	91.97	94.77

The marginal means plot of the effect of temperature is presented in Fig. 2(e). Variation in the temperature can be seen to exert a pronounced influence on the nickel deposition. Notice that the temperature has a positive main effect in this case; that is, increase in temperature enhances the average current efficiency. This observation is consistent with the experimental results plotted in Fig. 1(e). As has been pointed out before, since temperature has an adverse effect on the adsorption of ionic species (primary H^+) onto molybdenum disulfide particles, less MoS_2 powder is incorporated in the deposit at higher temperatures, thus increasing the nickel deposition efficiency.

Response contours

Response surface methodology is a collection of mathematical and statistical techniques that are useful for modelling and analysis of processes in which a response (performance measure) of interest is influenced by several variables [23]. To help visualize the shape of a response surface, the contours of the response surface are often plotted. The form of the relationship between response and independent variables is usually approximated by a polynomial within the range of the magnitudes of the respective independent variables that are investigated. The general approach of fitting equations to data is regression analysis [23]. Since it was desired to study the significant factors (pH and temperature) at three levels, an L9 orthogonal array was selected, which is shown in Table 6. If X_1 ($=(T-313)/15$) represents temperature and X_2 ($=(\text{pH}-2)/1.5$) represents pH, then the second order model that fits the current efficiency data is

$$Y = 0.5154 - 0.0551X_1 + 0.1836X_2 + 0.0506[3(X_1^2 - 2/3)] - 0.0301[3(X_2^2 - 2/3)] - 0.2694\ X_1X_2. \quad (1)$$

This equation can be used to predict the nickel deposition efficiency. Figure 3 shows the response

Table 6.
Orthogonal array for regression analysis of the current efficiency experiments

Run	Test sequence	pH	Temperature (K)	Current efficiency (%)
1	2	0.5	298	10.43
2	7	2	298	76.86
3	4	3.5	298	99.03
4	5	0.5	313	25.45
5	8	2	313	32.65
6	9	3.5	313	66.18
7	1	0.5	328	54.63
8	3	2	328	63.14
9	6	3.5	328	35.48

Current density = 200 A/m^2.
Rotation rate = 1000 r.p.m.
MoS_2 concentration in the bath = 50 kg/m^3.

contours as given by equation (1). Confirmation tests were conducted to validate this model. The response average of the confirmation tests was close to the predicted value, thus confirming the accuracy of the model.

Applicability of Guglielmi's model

The mechanism of electrocodeposition of inert particles and metals is far from well understood. One of the proposed models describing the codeposition of dispersed particles in metallic coatings is the Guglielmi's model [2]. The validity of Guglielmi's model for the codeposition of α-alumina and copper from copper sulfate plating baths [24] and graphite particles with chromium from chromium plating baths [25] has already been established. Guglielmi's model is based on two successive adsorption steps. In the first step, the particle, which is still surrounded by a layer of ions and solvent molecules, is at first only weakly adsorbed on the cathode, whereas in the second step, the electric field at the cathode strips the particles of the layer of surrounding ions, thus making the particles firmly bound to the cathode and subsequently embedded in the deposit. By a mathematical treatment of this process, the following expression was derived:

$$\frac{(1-\alpha)C}{\alpha} = \frac{Wi_0}{nFdv_0} e^{(A-B)\eta}\left(\frac{1}{K}+C\right), \qquad (2)$$

where C is the concentration of suspended particles in the bath expressed as volume percent, α is the volume fraction of particles in the deposit, W is the atomic weight of the deposited metal, n is the valency of the metal, F is the Faraday's constant, η is the overpotential and d is the density of the deposited metal. The parameters i_0 and A are related to the metal deposition, whereas parameters v_0 and B are related to the inert particle deposition. K is the adsorption constant which depends essentially on the intensity of the interaction between particles and electrode.

If the model is applicable to any composite electrodeposition system, a plot between $(1-\alpha)C/\alpha$ and C for different values of current i should give a set of straight lines converging at a point where $C = 1/K$. In order to test the validity of the mechanism proposed by Guglielmi for the codeposition of molybdenum disulfide and nickel from a basic Watts bath, different quantities of MoS_2 powder

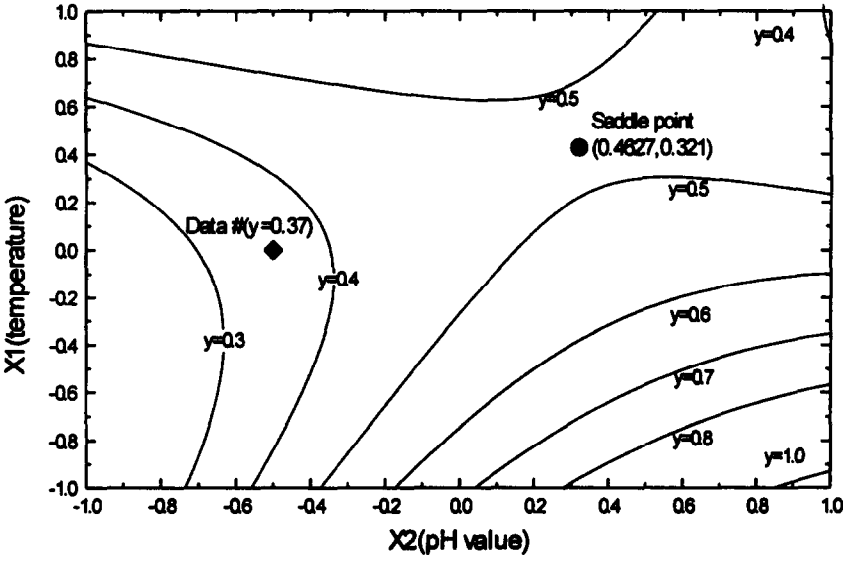

Fig. 3. Response surface contour plot.

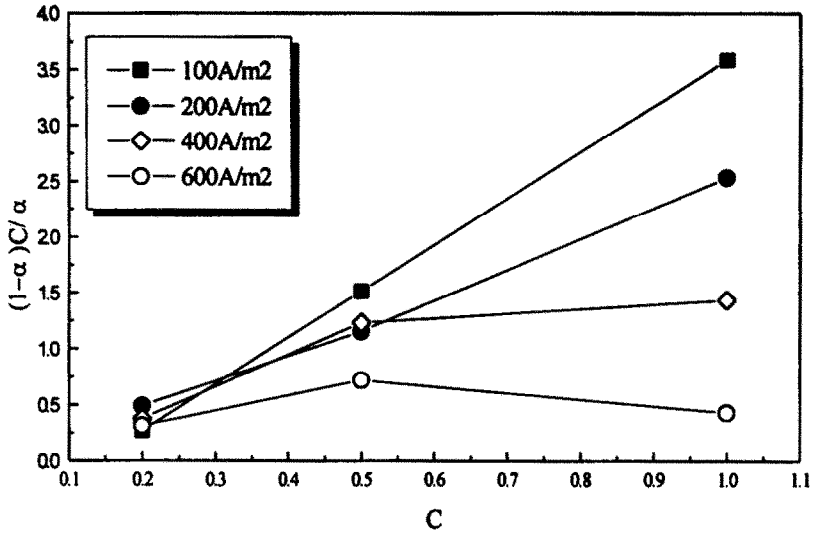

Fig. 4. Characteristics of the codeposition of MoS_2 particles and nickel from a Watts bath, according to equation (2).

particles were added to the basic Watts plating bath at the following conditions: temperature, 328 K; pH 2; and disc rotation rate, 1000 r.p.m. The results of these experiments are presented in Fig. 4, which shows the experimental data can be satisfactorily plotted as a set of straight lines, as required by equation (2), for the low current density cases (100 A/m^2 and 200 A/m^2), whereas codeposition behaviour of MoS_2 particles at high current densities (400 A/m^2 and 600 A/m^2) shows a different feature and does not obey Guglielmi's kinetic model. Similar results have also been reported for the electrodeposition of zinc-oxide particles composite at high current densities [26]. Further investigations of this phenomenon are presently being carried out in our laboratory.

CONCLUSIONS

The basic parameters (pH, temperature, current density, rotation rate, concentration of suspended particles, *etc.*) affecting the electrolytic codeposition of molybdenum disulfide with nickel have been characterized using statistical experimental design in this study. The weight percent of molybdenum disulfide in the deposit has been observed to be significantly affected by temperature and particles concentration in the bath. The temperature exerts an adverse effect, while the suspended particles concentration has a positive effect. pH and temperature have been observed to be significant factors affecting the current efficiency. Both these factors show positive main effect. A second order model which relates the current efficiency to the pH and temperature factors is also developed in this study. The agreement between the response average and the value predicted by the model is good. The physical model proposed by Guglielmi has been shown to be valid for the codeposition of molybdenum disulfide and nickel from a basic Watts bath at low current densities. The results at high current densities, however, do not obey Guglielmi's kinetic model, indicating the existence of a different operating mechanism. It has also been observed experimentally that the nickel deposition efficiency is lowered in the presence of molybdenum disulfide particles.

REFERENCES

1. J. R. Roos, J. P. Celis, J. Fransaer and C. Buelens, *JOM*, November, 60 (1990).
2. N. Guglielmi, *J. Electrochem. Soc.* **119,** 1009 (1972).
3. J. P. Celis, J. R. Roos and C. Buelens, *J. Electrochem. Soc.* **134,** 1402 (1987).
4. J. Fransaer, J. P. Celis and J. R. Roos, *J. Electrochem. Soc.* **139,** 413 (1992).
5. J. Fransaer, J. P. Celis and J. R. Roos, *Metal Finishing*, June, 97 (1993).
6. A. Hovestad and L. J. J. Janssen, *J. Appl. Electrochem.* **25,** 519 (1995).
7. M. Ghouse, M. Viswanathan and E. G. Ramachandran, *Metal Finishing*, November, 55 (1980).
8. H. Wendt and V. Plzak, in *Electrochemical Hydrogen Technologies—Electrochemical Production and Combustion of Hydrogen* (Edited by H. Wendt), p. 33, Elsevier, Amsterdam (1990).
9. Y. Y. Chang, M.S. Thesis, National Taiwan Institute of Technology, Taipei (1996).
10. E. A. Brandes and D. Goldthorpe, *Metallurgia*, November, 195 (1967).
11. M. Ghouse, M. Viswanathan and E. G. Ramachandran, *Metal Finishing*, April, 44 (1980).
12. G. N. K. R. Bapu, *Metal Finishing*, July, 37 (1994).
13. F. K. Sautter, *J. Electrochem. Soc.* **110,** 557 (1963).
14. S. R. Schmidt and R. G. Launsby, *Understanding Industrial Designed Experiments*, pp. 3–10, Air Academy Press, Colorado, U.S.A. (1994).
15. J. S. Yau and M. S. Liu, *Experimental Designs* (in Chinese), Ch. 1.5, Hwa-Tai Co., Taipei (1989).

16. M. Viswanathan and M. Ghouse, *Metal Finishing*, October, 67 (1979).
17. C. Buelens, J. P. Celis and J. R. Roos, *J. Appl. Electrochem.* **13,** 541 (1983).
18. Yu. V. Pleskov and V. Yu. Filinovskii, *The Rotating Disc Electrode*, p. 51, Consultants Bureau, New York (1976).
19. S. Voyutsky, *Colloid Chemistry*, p. 157, Mir Publishers, Moscow (1978).
20. D. Pletcher and F. C. Walsh, *Industrial Electrochemistry*, second edition, p. 70, Blackie Academic & Professional, U.K. (1993).
21. C. S. Tarn, H. T. Guo, S. L. Liu and H. S. Chang, *Principles and Technology of Electrodeposition* (in Chinese), p. 157, Tientsin Science and Technology Press, China (1993).
22. P. R. Webb and N. L. Robertson, *J. Electrochem. Soc.* **141,** 669 (1994).
23. G. E. P. Box and N. R. Draper, *Empirical Model-building and Response Surface*, John Wiley & Sons, U.S.A. (1987).
24. J. P. Celis and J. R. Roos, *J. Electrochem. Soc.* **124,** 1508 (1977).
25. R. Narayan and B. H. Narayana, *J. Electrochem. Soc.* **128,** 1704 (1981).
26. M. Kimoto, A. Yakawa, T. Tsuda and R. Kammel, *Metall.* **44,** 1148 (1990).